^{19}F NMR Studies of Fluorine-Labeled *Chromatium vinosum* High-Potential Iron Protein†

Dawei Li, Aileen Soriano, and J. A. Cowan*

Evans Laboratory of Chemistry, The Ohio State University, 120 West 18th Avenue, Columbus, Ohio 43210

Received September 1, 1995⊗

Fluorine-labeled analogues of *Chromatium vinosum* high-potential iron protein have been investigated by ^{19}F NMR spectroscopy. Fluorine-19 resonances have been assigned, and chemical shift variations, relaxation times, and temperature dependencies have been determined. Observed changes in fluorine chemical shifts and relaxation times following oxidation of the [Fe_4S_4] cofactor appear to reflect structural perturbation of the protein backbone and side chains, rather than variations in the paramagnetism of the cluster. Fluorine-19 NMR provides a probe of redox-dependent conformational change in electron-transfer proteins, which may also be of value for structural characterization of mutants. Evaluation of H_2O/D_2O solvent isotope effects on ^{19}F chemical shifts reflects solvent accessibility to various protein domains, while measurement of ^{19}F relaxation times affords a convenient test of the relative contribution of cross-relaxation to magnetization decay. For HiPIP, the results reported herein indicate that the cross-relaxation contribution to the longitudinal relaxation (T_1) is relatively small for both the oxidized and reduced states. Unusual temperature dependencies and fast relaxation times for the ^{19}F resonances of 3-F-Phe66 and 3-F-Tyr19 labeled HiPIP support a close interaction of these two residues with the iron−sulfur cluster.

Introduction

Iron−sulfur centers are important biological cofactors in both redox and nonredox biochemistry. An understanding of the functional properties of protein-bound iron−sulfur clusters requires detailed insight on the structure and dynamics of the surrounding polypeptide matrix. High-potential iron proteins (HiPIP's)[1] form a class of electron carriers that contain a [Fe_4S_4] cluster with redox potentials ranging from +450 to +50 mV.[1,2] Recently, the electronic properties of iron−sulfur centers have been the subject of intense study; however, the functional roles of individual residues remain uncertain. The cluster is surrounded by aromatic residues (Figure 1 and Table 1) that form a hydrophobic pocket and presumably help to define its physicochemical properties. It has been suggested that several of these residues might mediate electron transfer pathways,[1−3] although recent studies from our laboratory indicate other possibilities.[1]

In this paper we describe the use of ^{19}F NMR to investigate the chemistry of the buried aromatic core residues. By incorporation of specific fluorine-labeled amino acid residues, one can insert unique probes at well-defined locations within the protein core. We report the synthesis and purification of (2-, (3,- and (4-fluorophenyl)alanine (abbreviated 2-F-, 3-F-, and 4-F-Phe, respectively) and 5-fluorotryptophan (5-F-Trp) derivatives of *Chromatium vinosum* HiPIP, the assignment of ^{19}F NMR resonances, measurement of longitudinal relaxation times, and the temperature dependence of ^{19}F and ^{1}H resonances for native and fluorinated HiPIP. Related studies on the previously characterized 3-fluorotyrosine protein (3-F-Tyr) are also described.[4]

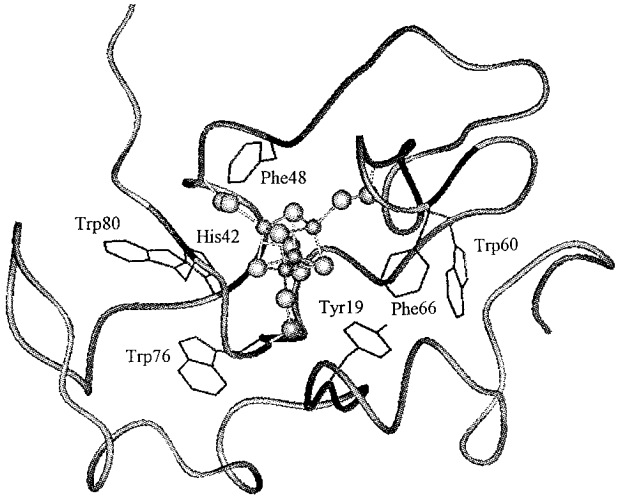

Figure 1. Structure of *C. vinosum* HiPIP, showing all of the aromatic side chains.

Table 1. Location of Aromatic Residues in Different HiPIP's[a,b]

HiPIP source	19	42	48(49)	60	66(67)	76	80
C. vinosum	Tyr	His	Phe	Trp	Phe	Trp	Trp
T. reseopersicina	Tyr	His	Phe	Trp	Phe	Trp	Trp
C. gracile	Tyr	His	Phe	Trp	Phe	Trp	Trp
T. pfennigii	Tyr	Phe	Phe	Trp	Phe	Trp	Trp
Rp. gelatinosa	Tyr	His	Lys(Phe)	Val	Phe	Trp	Trp
Paracoccus sp.	Tyr	Gln	Phe	Ser	Phe	Trp	Trp
E. halophila iso-1	Tyr	Lys	Phe	Trp	Phe	Trp	Tyr
E. halophila iso-2	Tyr	Lys	Phe	Trp	Phe	Trp	Tyr
Rs. tenue 3761	Tyr	Asn	Gln(Phe)	Ala	Ile(Pro)	Tyr	Tyr
Rs. tenue 2761	Tyr		Gln(Phe)	Ala	Ile(Pro)	Tyr	Phe

[a] Adapted from ref 32. [b] *C. vinosum* HiPIP numbering.

† Abbreviations: CR, cross relaxation; CSA, chemical shift anisotropy; EXSY, 2D exchange spectroscopy; HiPIP, high-potential iron−sulfur protein; IPTG, isopropyl-β-D-thiogalactopyranoside; NMR, nuclear magnetic resonance; NOESY, nuclear Overhauser effect correlated spectroscopy; TFA, trifluoroacetic acid; TMS, tetramethylsilane.

⊗ Abstract published in *Advance ACS Abstracts,* February 15, 1996.

(1) Agarwal, A.; Li, D.; Cowan, J. A. *Proc. Natl. Acad. Sci. U.S.A.* **1995**, *92*, 9440−9444.
(2) (a) Carter, C. W., Jr. In *Iron−sulfur Proteins III;* Lovenberg, W., Ed.; Academic Press: New York, 1977; pp 157−204. (b) Carter, C. W. Jr.; Kraut, J.; Freer, S. T.; Xuong, N. H.; Alden, R. A.; Bartsch, R. G. *J. Biol. Chem.* **1974**, *249*, 4212. (c) Mizrahi, I. A.; Meyer, T. E.; Cusanovich, M. A. *Biochemistry* **1980**, *19*, 4727.
(3) Bertini, I.; Gaudemer, A.; Luchinat, C.; Picioli, M. *Biochemistry* **1993**, *32*, 12887.
(4) Lui, S. M.; Cowan, J. A. *J. Am. Chem. Soc*. **1994**, *116*, 4483−4484.
(5) Agarwal, A.; Tan, J.; Eren, M.; Tevelev, A.; Liu, S. M.; Cowan, J. A. *Biochem. Biophys. Res. Commun.* **1994**, *197*, 1357.

0020-1669/96/1335-1980$12.00/0

Materials and Methods

Protein Purification. One liter of a cell culture carrying a high level expression system for either native or mutant *C. vinosum* HiPIP was grown in M9ZB medium at 37 °C to an OD ∼ 0.6−1.0.[5,6] The cell mass was pelleted at 3000 rpm for 10 min, resuspended in 1 L of M9 medium,[6] and expression induced by addition of IPTG (1 mM final concentration) followed by incubation at 37 °C for an additional 5 h. The cell mass was harvested, suspended in 10 mL of 20 mM Tris buffer (pH 7.0), and lysed by sonication. An equivalent volume of acetone (−20 °C) was added, and the mixture was centrifuged at 10 000 rpm for 15 min. The supernatant was diluted 3-fold with 10 mM NaCl solution and applied to a 2 × 10 cm DE-52 column equilibrated with 10 mM NaCl. The dark brown colored HiPIP was retained at the top of the column and was eluted with 150 mM NaCl solution. The fraction with Abs(283 nm)/Abs(388 nm) <2.9 was collected. Fluorine-labeled HiPIPs were obtained by inducing expression in a M9 medium supplemented with 100 mg/L of each amino acid, with the fluorinated derivative replacing the amino acid of choice.

NMR Sample Preparation. The purified protein was exchanged into 10 mM sodium phosphate buffer (pH 6.0, 0.03 M NaCl) by ultrafiltration (Amicon). The solution was reduced to a volume of ∼1.0 mL, lyophilized, and stored at 4 °C. Subsequently, the lyophilized sample was dissolved in either 0.5 mL D_2O (99.96% atom D, Aldrich) or in H_2O with 10% D_2O. The final sample contained 20 mM sodium phosphate and 0.06 M NaCl at pH 6.0. The concentration of ^{19}F-modified HiPIP was determined by comparing the peak intensity with standard 2-F-Phe or 5-F-Trp samples of known concentration. Partially oxidized HiPIP samples were prepared by adding small aliquots of a freshly prepared potassium ferricyanide solution (0.2 M) directly to the reduced protein sample in the NMR tube and checked by the appearance of the 1D ^{1}H NMR spectrum. Completely oxidized sample was prepared by addition of excess potassium ferricyanide and then removing residual ferricyanide by passing through a G-25 column equilibrated with an appropriate buffer and concentrating by ultrafiltration (Amicon).

NMR Spectroscopy. NMR spectra were acquired at 250.13 MHz for ^{1}H and 235.36 MHz for ^{19}F on a Bruker 250 AM spectrometer with an ASPECT 3000 data station. For ^{19}F NMR experiments, spectral widths were just sufficient (30 ppm average) to cover the region where peaks appear. All experiments were performed at 303 K. A total of 16K data points were used for 1D experiments. Fluorine-19 two-dimensional exchange experiments (EXSY) were recorded in phase-sensitive mode with the standard phase-sensitive NOESY pulse sequence.[7] In ^{19}F 2D EXSY experiments, 2K (t2 dimension) and 300 t1 increments were recorded with 64−128 transients per t1 increment. The t1 dimension was zero-filled to 1K data points, and a Lorentz-to-Gaussian window function with 10−20 Hz line broadening was applied to the FID in both dimensions prior to Fourier transformation. The T_1 relaxation times of ^{19}F peaks were measured by standard inversion recovery methods, both with and without ^{1}H broad-band decoupling. High-field ^{1}H spectra were referenced to TMS through the HOD resonance at 4.7 ppm, and ^{19}F spectra were referenced to TFA.

Theoretical Background. Fluorine-19 NMR is an exquisitely sensitive technique that can be applied to problems in structural and physical biochemistry. This arises for two principal reasons. First, the ^{19}F nucleus ($I = {}^1/_2$) shows a similar sensitivity (∼83%) to that of ^{1}H, and second, the chemical shift range is large. Furthermore, substitution with fluorinated amino acids does not usually result in significant changes in protein structure or activity.[8−10] Gerig has prepared an extensive review of fluorine NMR studies of proteins that summarizes and discusses many of the important issues that need to be considered in application of this technique.[24b] Fluorine is usually introduced via the aromatic rings of Phe, Trp, and Tyr residues, since fluorinated derivatives of these amino acids are commercially available at reasonable cost. The effects of fluorine substitution for aromatic hydrogen are generally small or undetectable.

***T*$_1$ Measurements and Evaluation of Cross-Relaxation (CR).** The longitudinal relaxation mechanism for ^{19}F nuclei in this paramagnetic Fe−S protein comprises contributions from three major sources: namely, ^{19}F−^{1}H dipolar relaxation, ^{19}F chemical shift anisotropy (CSA), and paramagnetic relaxation from the dipolar interaction of ^{19}F with unpaired electron spin on the [Fe_4S_4] cluster. There may be an exchange contribution to the relaxation in mixtures of the oxidized and reduced protein; however, this is eliminated in samples containing only (i.e. ≥99%) the oxidized or reduced form. The significance of the CSA contribution to relaxation depends on the magnetic field strength and the protein correlation time (τ_c). CSA is independent of the field strength when $\omega_o\tau_c > 1$, and under these circumstances the contribution of CSA to the magnitude of the relaxation time T_1 is negligible.[11] It has long been recognized that cross-relaxation (CR) of heteronuclear (e.g. ^{19}F, ^{15}N, ^{13}C) spin magnetization to the dipolar coupled ^{1}H spins contributes to the overall relaxation mechanism of the heteronuclear spin. Cross-relaxation (CR) is the result of mutual spin flipping in pairs of dipolar-coupled spins, and depends on the correlation time of the molecule and the separation of the interacting spins. The CR contribution to the relaxation of distinct spins (in this case ^{19}F) is defined by eq 1, where I and I° are the magnetization of the distinct spins X

$$d(I_x)/dt = -(\varrho_x + \varrho_p + \sigma_{XH})(I_x - I_x^0) + \sigma_{HX}(I_H - I_H^0) \quad (1)$$

or H at time t or at thermal equilibrium ($t = 0$), respectively, ρ_x and ρ_p are the relaxation rates from diamagnetic and paramagnetic sources, respectively, and σ_{HX} ($=\sigma_{XH}$) is the cross relaxation rate between spins X and H. For heteronuclear systems, a single exponential time dependence of the longitudinal magnetization of each heteronuclear spin can be achieved by continuous saturation of the other spin-type.[14] However, it has been reported that for a ^{19}F−^{1}H dipolar coupled spin system, where a single ^{19}F spin is coupled with a group of ^{1}H spins in a protein, the single exponential decay of ^{19}F magnetization will hold, even without ^{1}H irradiation.[17] The contribution of cross-relaxation to the overall relaxation of ^{19}F under strongly paramagnetic conditions has not previously been examined but can be estimated in our ^{19}F−^{1}H coupled spin system by comparing relaxation times measured with and without continuous ^{1}H decoupling.

Estimation of ^{19}F-Cluster Distances by Relaxation Measurements. Relaxation of ^{19}F nuclei that lie adjacent to the paramagnetic cluster is dominated by dipolar rather than contact interactions with the cluster. The distances between the paramagnetic center and selected ^{19}F nuclei can be estimated by use of the Solomon eq.[18] This approach has been used extensively in chemical and biochemical studies.[19,20] By substitution of nuclear parameters appropriate for the ^{19}F nucleus, and omission of the contact contribution, the Solomon eq can be simplified to the form of eq 2, where T_{1p} is the paramagnetic contribution to the observed

$$1/T_{1p} = C^6/r^6 \quad (2)$$

relaxation time, C = 9.32 Å $s^{-1/6}$ for oxidized HiPIP with total spin $S = {}^1/_2$, and r is the distance from the fluorine nucleus to the cluster center (point dipole assumption). For nuclei that lie close to the cluster the point dipole approximation is less satisfactory and it is necessary

(6) Studier, F. W.; Rosenberg, A. H.; Dunn, J. J.; Dubendorff, J. W. *Methods Enzymol.* **1990**, *185*, 60−89.
(7) Bodenhausen, G.; Kogler, K.; Ernst, R. R. *J. Magn. Reson.* **1984**, *58*, 370.
(8) (a) Luck, L. A.; Falke, J. J. *Biochemistry* **1991**, *30*, 4248. (b) Luck, L. A.; Falke, J. J. *Biochemistry* **1991**, *30*, 6484.
(9) Gregory, D. H.; Gerig, J. T. *Biopolymers* **1991**, *31*, 845.
(10) Drake, S. K.; Bourret, R. B.; Luck, L. A.; Simon, M. I.; Falke, J. J. *J. Biol. Chem.* **1993,** *268*, 13081 and references therein.
(11) Hull, W. E.; Sykes, B. D. *J. Mol. Biol.* **1975**, *98*, 121.
(12) Granot, J. *J. Magn. Reson.* **1982**, *49*, 257.
(13) Andree, P. J. *J. Magn. Reson.* **1978**, *29*, 419.
(14) Campbell, I. D.; Freeman, R. *J. Magn. Reson.* **1973**, *11*, 143.
(15) Sletten, E.; Jackson, J. T.; Burns, P. D.; La Mar, G. N. *J. Magn. Reson.* **1983**, *52*, 492.
(16) La Mar, G. N.; de Ropp, J. S. In *Biological Magnetic Resonance*; Berliner, L. J., Reuben, J., Eds.; Plenum Press: New York, 1993; Vol. 12, pp 1−78.
(17) Hull, W. E.; Sykes, B. D. *J. Chem. Phys.* **1975**, *63*, 867.
(18) Solomon, I. *Phys. Rev.* **1955**, *99*, 559.
(19) Bertini, I.; Luchinat, C. *NMR of Paramagnetic Molecules in Biological Systems*; Benjamin/Cummings: Menlo Park, CA, 1986; p 36.
(20) Dwek, R. In *Nuclear Magnetic Resonance (N.M.R.) in Biochemistry*; Clarendon Press: London, 1973; Chapter 2, p 12.

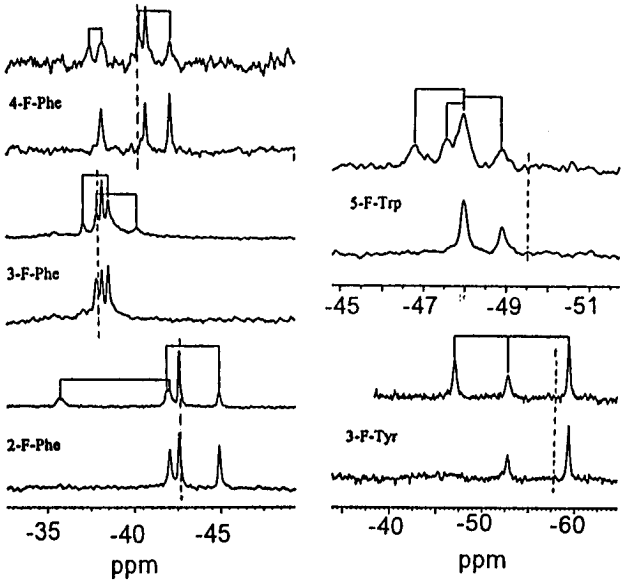

Figure 2. ^{19}F NMR spectra of fluorine-labeled HiPIP. Two spectra are shown for each fluorinated amino acid. The lower spectrum is recorded in the reduced state, while the upper spectrum is obtained from a mixture of the reduced and oxidized states with each redox pair connected by lines. The vertical dashed lines indicate the ^{19}F chemical shift position of free-fluorinated amino acids.

to consider the individual contributions from each iron. With the assumption that the electron density is equally averaged over each iron site, the modified relaxation eq 3 can be written. In the limit where a

$$1/T_{1p} = (C')^6 \sum_{i=1}^{4} 1/r_i^6 \qquad (3)$$

nucleus lies close to van der Waals contact with a specific iron center, the contribution from the remaining ions to paramagnetic relaxation is less than 10%. For intersite distances of ≥ 7 Å the difference in estimated paramagnetic relaxation using either eq 2 or 3 is $\leq 12\%$.

Results

Characteristics of Fluorinated HiPIP. The incorporation efficiency of fluorinated amino acids was determined by integrating the ^{19}F resonances in a sample of the F-labeled HiPIP relative to a fluorinated amino acid of known concentration. The protein concentration was established by absorbance measurements. The incorporation efficiencies were 22%, 38%, and 32% for 2-F, 3-F, and 4-F-Phe, respectively, 64% for 3-F-Tyr, and around 10% for 5-F-Trp. No heterogeneity was observed during ion-exchange chromatographic purification of these labeled proteins, while the optical characteristics and reduction potentials were also found to be similar for the native and fluorinated samples. There is, therefore, no evidence for heterogeneity in either the structural or physicochemical properties of these labeled proteins relative to native HiPIP. Irrespective of the extent of incorporation, the ^{19}F NMR experiments target the labeled protein molecules and afford a probe of structural and dynamics issues.

^{19}F NMR of Fluorinated HiPIP. ^{19}F NMR spectra of 2-, 3-, 4-F-Phe, 3-F-Tyr, and 5-F-Trp HiPIP were recorded under similar experimental conditions and are shown in Figure 2. In each case the lower spectrum shows the reduced protein, while the upper spectrum was obtained from a mixture of reduced and oxidized forms with an ox:red ratio of approximately 1:1. The vertical dashed lines represent the position of ^{19}F frequencies for the free fluorinated amino acids. It is clear that the ^{19}F frequencies in the completely reduced form do not change in the mixture, and neither do the resonances from the completely

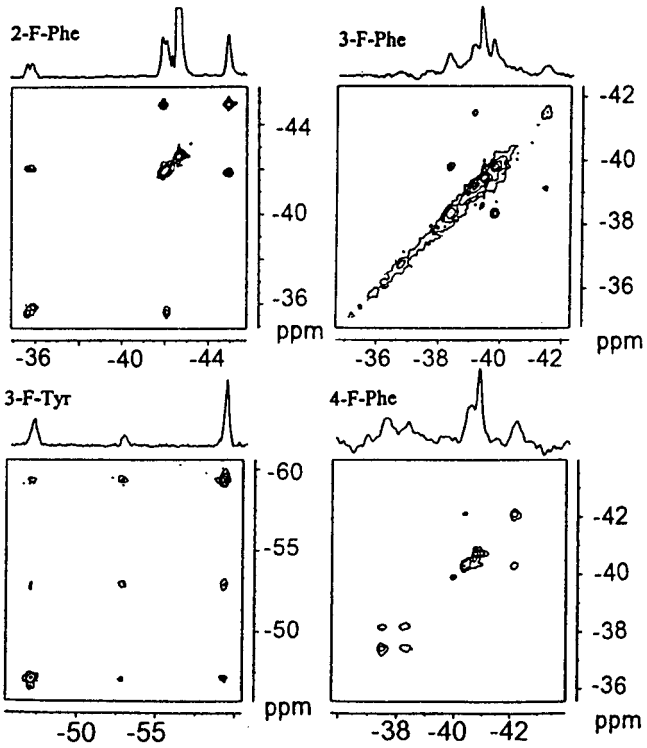

Figure 3. Two-dimensional ^{19}F EXSY spectra of fluorinated HiPIP obtained from a 1:1 mixture of reduced:oxidized HiPIP. These spectra correlate signals in the reduced and oxidized states that derive from the same nucleus.

oxidized form (not shown). This indicates that the ferricyanide and ferrocyanide ions present in solution have no detectable influence on the chemical shifts of these fluorine centers. There is an intense peak in the spectrum of each of the (fluorophenyl)-alanine HiPIP derivatives. This peak does not change in intensity upon oxidization, has no redox partner (Figure 2), and displays a much longer T_1 relaxation time (from 0.4 to 0.8 s). This peak arises from the additional N-terminal Phe residue (residue number -1) introduced during construction of the synthetic HiPIP gene in the pET-21d(+) expression vector.[5] It is clear that almost all other ^{19}F peaks are shifted after oxidation (Figure 2). All shifts are downfield except for one of the 3-F-Phe peaks that shifts upfield. The redox pairs indicated in Figure 2 were established by the ^{19}F 2D EXSY spectra shown in Figure 3.

In the EXSY experiments, the mixing times were calculated according to the spin−lattice relaxation time of each resonance and the electron self-exchange rates of native HiPIP.[21] The second-order electron self-exchange rate constant (3.0×10^4 M^{-1} s^{-1}) of the native HiPIP was estimated from EXSY spectra of the hyperfine-shifted ^{1}H resonances for a variety of mixing times and is in good agreement with earlier data obtained from T_1 measurements (1.7×10^4 M^{-1} s^{-1}).[22] In this paper the purpose of the EXSY experiment was simply to establish the connectivity between fluorine resonances in the reduced and oxidized forms, and so we selected the self-exchange rate of native HiPIP to allow estimation of the appropriate mixing time for the experiment. The mixing times used in this EXSY experiment are 10 ms for 3-F-Tyr, 8 ms for 4-F-Phe, 9 ms for 3-F-Phe, and 15 ms for 2-F-Phe.

Variable-temperature experiments were performed on the fully reduced and fully oxidized fluorine-labeled HiPIP's. With

(21) Perrin, C. L.; Dwyer, T.-J. *Chem. Rev.* **1990**, *90*, 935.
(22) Sola, M.; Cowan, J. A.; Gray, H. B. *J. Am. Chem. Soc.* **1989**, *111*, 6627.
(23) Hull, W. E.; Sykes, B. D. *Biochemistry* **1974**, *13*, 3431.

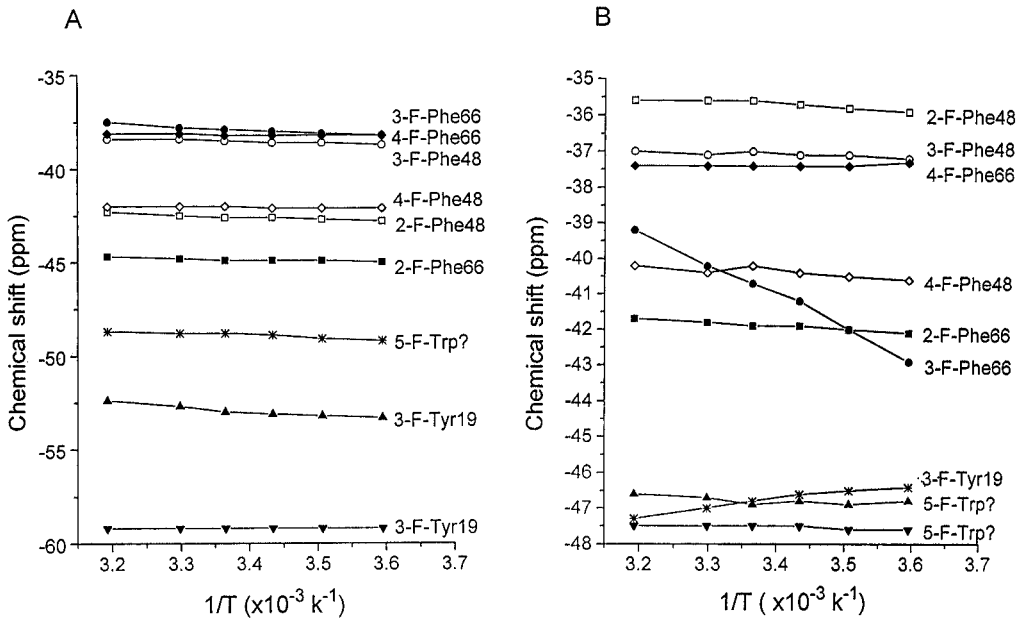

Figure 4. Temperature dependence of the ^{19}F resonances in the reduced (A) and oxidized (B) states.

Table 2. Comparison of ^{19}F Relaxation Times Estimated by Different Methods and in Different Redox States

assgnt[a]	resonance (ppm)	T_{1obs} (s)[b]	assgnt[a]	resonance (ppm)	T_{1obs} (s)[b]
2-F-Phe48	−42.0, red	0.076	4-F-Phe48	−42.1, red	0.19
	−35.6, ox	0.065		−40.3, ox	0.6
2-F-Phe66	−44.9, red	0.108	4-F-Phe66	−38.2, red	0.030
	−41.9, ox	0.109		−37.4, ox	0.10
3-F-Phe48	−38.5, red	0.25	3-F-Tyr19	−52.9, red	0.036
	−37.1, ox	0.23		−59.3, red	0.044
3-F-Phe66	−37.9, red	0.048		−47.1, ox	0.057
	−40.2, ox	0.037			

[a] Assignments are made on the basis of the relaxation times and comparison of the distances evaluated from relaxation rates and crystallography and were confirmed by mutagenesis experiments (Phe48H/R) as illustrated in Figure 7. [b] Similar T_1 values were measured with and without ^{1}H decoupling and from the initial slope of a semilogarithmic T_1 plot, where $\ln((I^\circ - I_t)/(2I^\circ))$ is plotted as a function of the delay time t, I° is the intensity at equilibrium and I_t is the intensity at delay time t. Errors are estimated at ±7%. These arise principally from the precison in measuring peak intensities and represent the variation observed between different experiments (i.e., the reproducibiltiy of the data). For any single data set the actual fits were extremely good.

the exception of the redox pair corresponding to 3-F-Phe66 (Figure 4; the justification for specific assignments is made later in the text), and 3-F-Tyr19 in the oxidized protein, there is no significant temperature dependence of resonance frequencies or line widths over the range from 5 to 40 °C. At each temperature, the two (fluorophenyl)alanines, and the three fluorotryptophans in labeled HiPIP, give rise to only one ^{19}F resonance per residue. For the case of 3-F-Tyr (Figure 2), the aromatic ring appears to rotate slowly in the reduced form, but faster in the oxidized form,[4] which is consistent with a close contact interaction between Tyr-19 and the reduced cluster.

Fluorine-19 T_1 relaxation times were measured for the fully reduced and fully oxidized samples by standard inversion recovery methods, using a delay time of 2.0−3.0 s. Table 2 summarizes longitudinal relaxation times evaluated from these measurements and obtained from three distinct sets of experimental conditions. The multiplicity of ^{19}F resonances observed for the free fluoroamino acids was observed to disappear when spectra were recorded with ^{1}H decoupling, resulting in singlet peaks with narrow line widths. This experiment was used to check the decoupling efficiency. Relaxation times were determined without continuous ^{1}H decoupling, with ^{1}H decoupling over the entire pulse experiment, and from the initial slope of a semilogarithmic plot obtained without ^{1}H decoupling. Within experimental error, similar values were observed by each method, and so the cross-relaxation (CR) contribution to T_1 is relatively small for both the oxidized and reduced states of the protein. In each case the magnetization decay curves could be reasonably fit to a single exponential for evaluation of T_1's. It should be noted that the relaxation times for two resonances, from 3-F-Phe48 and 4-F-Phe48, are unusually long in the reduced form and even longer in the oxidized form. This most likely arises from increased solvent exposure in the oxidized state. Fluorine-19 relaxation times for free fluorinated amino acids are 2.62, 3.08, and 4.04 s for (2-, (3-, and (4-fluorophenyl)-alanines, respectively. No complications were expected in the measurement of T_1 values as a result of electron self-exchange between the reduced and oxidized forms, since relaxation measurements were made on samples that contained either oxidized or reduced HiPIP but not mixtures of both forms.

When spectra were acquired with continuous broad-band proton decoupling, the observed NOE for the ^{19}F resonances was found to be small for the F-Phe derivatives in both reduced and oxidized HiPIP (Figure 5). We shall later demonstrate that this arises from the low efficiency of cross relaxation relative to the paramagnetic contribution to relaxation. Also, we observed a slight change in line widths for the ^{19}F resonances for spectra obtained with and without ^{1}H decoupling.

The distances from ^{19}F to the center of the cluster were evaluated for the oxidized form by use of eq 2. In this evaluation, the average relaxation time of the resonance from the 5-fluorotryptophan residues (Figure 2) was chosen as the diamagnetic relaxation time T_{1d}. From the three 5-F-Trp resonances (with T_1's estimated as 0.21, 0.29, and 0.25 s) an average relaxation time of 0.25 s was selected. The relaxation times for the 5-F-Trp resonances were found to be similar for the reduced protein since all three Trp residues are located far from the cluster (>10 Å), and so there is no significant paramagnetic relaxation contribution. Also, the tumbling times of the interior Trp and Phe residues are assumed to be similar, and so the diamagnetic and CR contributions to ^{19}F relaxation will be similar for the fluorotryptophan and (fluorophenyl)-

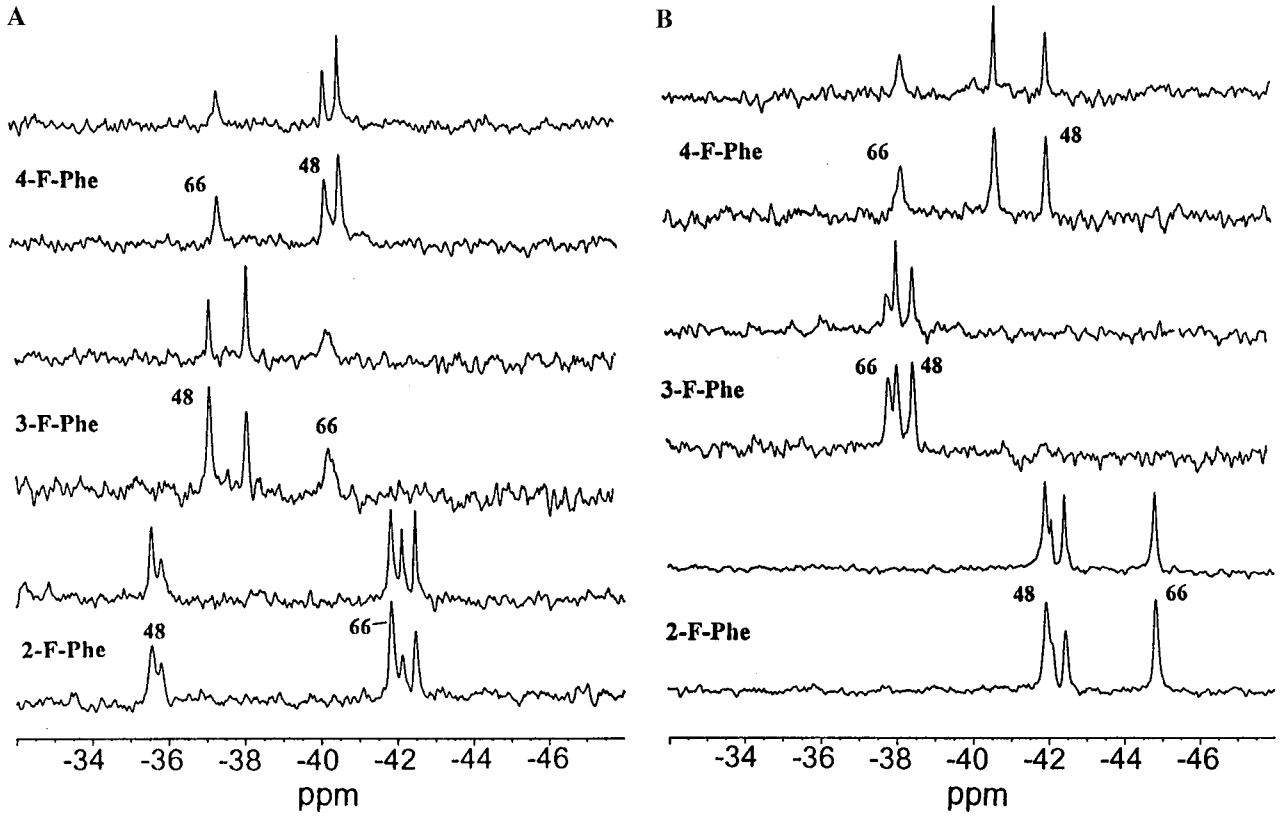

Figure 5. ^{19}F NOE with ^{1}H irradiation in the oxidized (A) and reduced (B) forms of fluorine-labeled HiPIP. For each pair, the lower spectrum was collected without proton decoupling, while the upper spectrum was obtained with broad-band proton decoupling for the entire spectral measurement. The integrated intensities are in line with the ratio's calculated theoretically and listed in Table 6.

alanine residues. Such an assumption is reasonable and in any case is less critical for the comparison of T_1 than for T_2 values. The paramagnetic relaxation time T_{1p} can be estimated by use of eq 4, where T_{1obs} is the observed relaxation time (Table 2)

$$1/T_{1p} = 1/T_{1obs} - 1/T_{1d} \quad (4)$$

and T_{1d} is the relaxation time in the diamagnetic limit. The ^{19}F relaxation contribution from dipolar interactions with neighboring ^{1}H nuclei has not been included in T_{1p} since values for T_{1obs} were obtained either with ^{1}H decoupling or the initial slope method, and so we can take $(1/T_{1obs} - 1/T_{1d})$ as the paramagnetic relaxation time. The distances obtained from the X-ray structure (r_{c1} and r_{c2}) and evaluated from the relaxation measurements (r_{r1}) are compared in Table 3 for oxidized HiPIP. X-ray distances were measured from the protons (substituted by ^{19}F) to the center of cluster. Distances for 2-F-Phe, 3-F-Phe, and 3-F-Tyr HiPIP have two possible values (r_{c1}, r_{c2} and their average r_{c3}). The relaxation derived distances for oxidized 2-F-Phe and 3-F-Phe derivatives are in reasonable agreement with average X-ray distances and support the idea of fast rotation for the aromatic rings. Discrepancies for 3-F-Phe66 and 3-F-Phe48 are discussed below. At this point, we tentatively assigned all F-Phe resonances by comparing the crystallographically determined distances with estimates from relaxation measurements (Table 3). These assignments were verified by site-directed mutagenesis experiments by mutation of residue Phe48 to His or Arg and expressing the mutant protein in a minimal medium containing specific isomers of (fluorophenyl)-alanine. Each of the ^{19}F resonance assignments made for Phe48 in native HiPIP were observed to disappear in the mutant proteins (Figure 7). The assignments of Phe66 were consequently obtained by inspection. We did not attempt to estimate the relaxation based distances for the three tryptophan sites in 5-F-Trp HiPIP (average relaxation time 0.25 s), since the average distance from ^{19}F to the center of the cluster is over 10 Å. Also, assignment of specific resonances to F-Trp residues was hampered by severe signal overlap, which was not alleviated by collecting spectra at either higher or lower temperatures.

Solvent exposure of Phe48 resulted in significant nonparamagnetic contributions to T_{1obs}. As described earlier, this tends to increase T_{1obs} values such that $T_{1obs} \sim T_{1d}$ for the 3,4-F-Phe48 resonance in oxidized and reduced HiPIP, while the significant increase in apparent T_{1p} accounts for the overestimation of $^{19}F-$ cluster distance for the 3-F-Phe48 position noted in Table 3. In contrast, the apparent underestimation of the distance in the case of 3-F-Phe66 is due to the inadequacy of the point dipole approximation used in eq 2. Since carbon-3 of Phe66 lies close to the cluster, there is a disproportionate influence from one iron center when the fluorine is oriented most closely to the cluster, and so it is necessary to use an eq such as (3), where the contributions from each iron are summed. Assuming an equal distribution of electron density over all four iron sites, and that the three remaining iron sites lie at a distance 2.5 Å further than that neighboring the nucleus of interest, a distance of ~5.0 Å to the proximal iron is estimated. This is in good accord with the crystallographic value of ~4.7 Å. In fact the slight over estimate of the distance reflects the averaging influence of the other conformer of the 3-F-Phe66 where the ^{19}F-center lies away from the cluster and relaxation is promoted less efficiently.

The influence of solvent isotope effects[24] on the fluorine chemical shifts was examined in samples of both the fully reduced and oxidized forms. In the reduced form, only the peak from Phe(−1) in the F-Phe HiPIP samples showed a significant

(24) (a) Gerig, J. T. *Biol. Magn. Reson.* **1978**, *1*, 139. (b) Gerig, J. T. *Prog. Nucl. Magn. Reson.* **1994**, *26*, 293.

Table 3. (A) ^{19}F Chemical Shifts, T_{1p} Relaxation Rates, Evaluation of ^{19}F -Cluster Intersite Distances, and Estimation of Dipolar Shifts for Oxidized HiPIP and (B) ^{19}F Chemical Shifts and T_{1p} Relaxation Rates for Reduced HiPIP

(A) oxidized F-HiPIP

residues	$\delta(^{19}F)^a$	T_{1p} (s)^b	r_{r1} (Å)^c	r_{c1} (Å)^d	r_{c2} (Å)	r_{c3} (Å)	$\delta_{dip}{}^e$
2-F-Phe48	−35.6	0.088	6.2	5.1	7.5	6.3	1.46
2-F-Phe66	−41.9	0.192	7.0	5.5	8.9	7.2	0.98
3-F-Phe48^f	−37.1	2.63	10.8	6.8	8.7	7.8	0.76
3-F-Phe66^f	−40.2	0.043	5.5	5.7	9.0	7.4	0.90
4-F-Phe48	−40.3			8.4	8.4	8.4	0.62
4-F-Phe66	−37.4	0.167	6.8	7.6	7.6	7.6	0.82
3-F-Tyr19	−47.1	0.074	6.0	5.6	8.6	7.1	1.02

(B) Reduced F-HiPIP

residues	$\delta(^{19}F)^a$	T_{1p} (s)^b	residues	$\delta(^{19}F)^a$	T_{1p} (s)^b
2-F-Phe48	−42.0	0.109	4-F-Phe48	−42.1	0.769
2-F-Phe66	−44.9	0.189	4-F-Phe66	−38.2	0.034
3-F-Phe48	−38.5		3-F-Tyr19	−52.9	0.042
3-F-Phe66	−37.9	0.059		−59.3	0.053

^{a} ^{19}F chemical shifts for protein-bound fluorinated residues (ppm). The uncertainty is ±0.02 ppm. Chemical shifts (relative to TFA) for the free amino acids are as follows: −58.0 ppm for 3-F-Tyr, −42.6 ppm for 2-F-Phe, −37.9 ppm for 3-F-Phe, −40.3 ppm for 4-F-Phe, and −49.5 ppm for 5-F-Trp. ^{b} Paramagnetic relaxation rates (=$1/T_{1p}$) were calculated from eq 4, using T_{1obs} from Table 2, where T_{1d} is the average relaxation time for 5-F-Trp in the oxidized state (0.25 ± 0.02 s). Errors can be estimated from the error limits for T_{1obs} listed in Table 2, and the error just cited for T_{1d}. ^{c} r_{r1} (±0.2 Å) for the oxidized form was calculated from eq 2, with constant $C = 9.32$ Å s$^{-1/6}$ for ^{19}F and $S = {}^1/_2$ at room temperature. For the 4-F-Phe resonance at −40.3 ppm, the value of $(1/T_{1obs} - 1/T_{1d}) < 0$ is unreasonable and is regarded as a special case. ^{d} Distances (r_{c1} and r_{c2}) were measured from the X-ray structure of oxidized HiPIP. There are two possible locations (r_{c1} and r_{c2}) for each ^{19}F (except for 4-F-Phe), and the distances are from ^{19}F to the center of the cluster. r_{c3} is the average of r_{c1} and r_{c2}. ^{e} The crystallographically determined distances (r_{c3}) were used to calculate the dipolar shift (δ_{dip}) for the oxidized form. ^{f} As discussed in the text, the agreement between the calculated and crystallographic distances is poor. For 3-F-Phe66, reasonable agreement is obtained by use of eq 3.

downfield shift (an average $\Delta\delta \sim 0.11$ ppm) when the solvent changed from D_2O to H_2O (Table 5). Apparently, with the sole exception of the additional N-terminal Phe, the inner aromatic residues in the cluster pocket are not solvent exposed.[25] In the oxidized state, the isotopic shift is greater than 0.1 ppm for 3-F-Phe48 and 4-F-Phe48. This correlates with observations from relaxation measurements, with $T_1 \sim 0.23$ s for the former, and $T_1 \sim 0.6$ s for the latter, and suggests that these two sites are differentially exposed to solvent with a corresponding increase in relaxation times. Isotope-induced chemical shift changes of less than 0.1 ppm are not considered significant; however, shifts greater than 0.1 ppm correspond to a frequency change of greater than 23.5 Hz, which is readily detectable and is significant.

^{1}H NMR of Fluorinated HiPIP. Only the ^{1}H resonances in the spectrum of the oxidized 3-F-Tyr derivative show significant shifts relative to the spectrum of native HiPIP (Figure 6). No shifts were observed in the spectra for reduced 3-F-Tyr HiPIP nor in the spectra for the (fluorophenyl)alanine or fluorotryptophan derivatives in either the oxidized or reduced states (spectra not shown). The assignments, T_1 relaxation times, and shifts of the signals in oxidized 3-fluorotyrosine HiPIP are listed in Table 4. The signals for native HiPIP (labeled in Figure 6A) can be easily identified by comparing the resonance

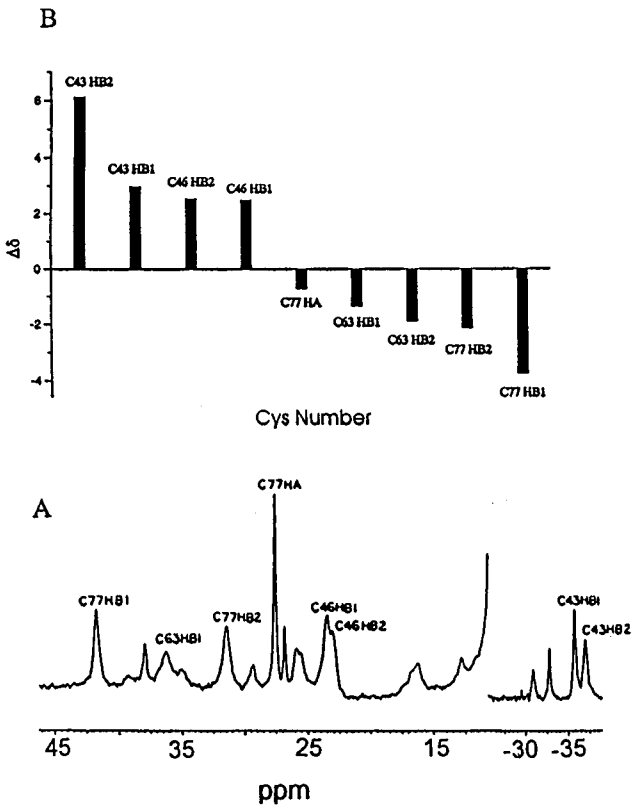

Figure 6. (A) ^{1}H NMR spectrum of hyperfine-shifted signals in a mixture of native (peaks assigned) and 3-F-Tyr HiPIP. (B) Differences of chemical shifts ($\Delta\delta = \delta^N - \delta^F$) between native ($\delta^N$) and fluorinated ($\delta^F$) HiPIP.

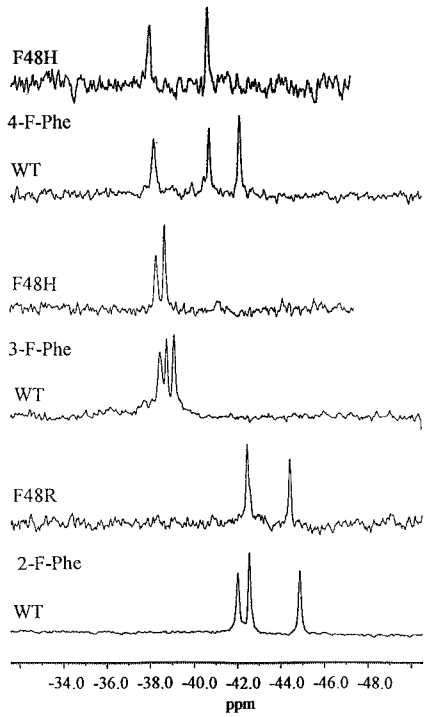

Figure 7. Comparison of the ^{19}F NMR spectra for wild type (WT) and Phe48 HiPIP mutants. The ^{19}F resonances from F-Phe48 disappear in spectra from the mutant protein. Assignments are summarized in Tables 2 and 3.

frequencies with the published assignments.[26−29] The signals for fluorinated HiPIP can be assigned from the shift pattern. It

(25) Hansen, P. E.; Dettman, H. D.; Sykes, B. D. *J. Magn. Reson.* **1985**, *62*, 487.

(26) Bertini, I.; Brigaanti, F.; Luchinat, C.; Scozzafava, A.; Sola, M. *J. Am. Chem. Soc.* **1991**, *113*, 1237.

Table 4. Comparison of ^{1}H NMR Chemical Shifts and Longitudinal Relaxation Times between Native and 3-F-Tyr HIPIP in the Oxidized Form

signal[a]	native δ, ppm	fluoro deriv δ ppm	δ(nat) − δ(fluor) ppm	T_1^{nat} (ms)	T_1^{fluoro} (ms)
Cys77 CHβ(1)	37.92	41.68	−3.76	12	13
Cys77 CHβ(2)	29.30	31.45	−2.15	7.7	7.1
Cys77 CHα	26.78	27.51	−0.73	32	39
Cys63 CHβ(1)	35.15	36.50	−1.35	3.4	3.7
Cys63 CHβ(2)	104.9	106.8	−1.90		
Cys46 CHβ(1)	25.88	23.41	+2.47	13	8.8
Cys46 CHβ(2)	25.56	23.03	+2.53	7.0	6.8
Cys43 CHβ(1)	−32.82	−35.79	+2.97	26	22
Cys43 CHβ(2)	−30.92	−37.04	+6.12	8.9	11

[a] Assignments from ref 27.

was also noted that the temperature dependence of the hyperfine shifts (not shown) are very similar for native and 3-F-Tyr HiPIP.

Discussion

^{19}F Chemical Shift. The chemical shifts of the free fluorine substituted amino acids are indicated by a vertical dashed line in Figure 2. It is clear that the ^{19}F resonances for all substituted amino acids in HiPIP are shifted relative to the free amino acids and are readily distinguished in both the reduced and oxidized states (Table 3 and Figure 2). It is well-known that ^{19}F chemical shifts are very sensitive to the local environment. It is clear from Figure 2 that the shifts from the protein-bound fluorinated amino acids are scattered. In part this may arise from the dipolar or contact shift from the paramagnetic cluster. At room temperature both the reduced and the oxidized states are paramagnetic. The oxidized state has a formal spin of $^1/_2$, while the reduced state exhibits a residual spin as a result of thermal population of electronic excited states. The paramagnetic dipolar shift depends not only on the distance (r^{-3}) between the electron spin and the fluorine nucleus, and the orientation (θ) of the inter-site vector relative to the direction of the electron spin dipole, but also depends on the anisotropic g-values of the electron spin as shown in eq 5, where δ_{dip} is the dipolar shift in

$$\delta_{dip} = (\kappa/Tr^3)(3\cos^2\theta - 1)(g_{||}^2 - g_{\perp}^2) \qquad (5)$$

ppm, κ is a constant, T is the temperature, and r is the distance from the nucleus of interest to the paramagnetic center.[19] As a result, the ^{19}F nuclei may show a paramagnetic dipolar shift as a result of the net electron spin on the cluster. However, it is difficult to interpret the results shown in Figure 2 in general terms. Comparison of spectra for the reduced and oxidized states shows a downfield shift following cluster oxidation for all but one pair of ^{19}F signals (corresponding to Phe66) in (3-fluorophenyl)alanine HiPIP. Since the paramagnetic dipolar shift is temperature dependent,[19] the small or negligible temperature dependence of the chemical shift for the other ^{19}F nuclei in both reduced and oxidized states (Figure 4) may indicate that the contribution of the dipolar shift is small. An *upper limit* for the magnitude of the dipolar shift can be readily estimated for the oxidized cluster by use of eq 5. The g-values for oxidized HiPIP are $g_{||} = 2.12$, $g_{\perp} = 2.04$,[30] and upper limits for the dipolar shifts (maximum when $\cos^2\theta = 1$) range from 0.62 to 1.46 ppm at 298 K (Table 3), assuming $S = {}^1/_2$. The calculation of the pseudocontact shift contribution was carried out only to provide an estimate of the upper limit of this contribution and not to evaluate realistic values of the shifts per se. In fact we estimate the dipolar shifts for the oxidized state to be relatively small, and these will be even less significant for the reduced cluster. The observed ^{19}F shifts are much larger and allow us to conclude that the difference in chemical shifts observed for reduced and oxidized HiPIP are most likely diamagnetic in origin and arise from local structural or conformational changes of the polypeptide chain rather than spin state changes on the cluster. In turn, this implies that ^{19}F is a valuable structural tool for monitoring structural perturbations arising from a change of cluster redox state.

The fluorinated amino acids do not significantly influence the electronic structure of the cluster. Also, spin−lattice relaxation times for the hyperfine-shifted protons do not change significantly and show no obvious trend in the small perturbation that is observed (Table 4). In contrast, the ^{19}F resonances from 3-F-Phe 66 HiPIP (−37.9 ppm in the reduced and −40.2 ppm in oxidized forms) do display highly unusual behavior. Relative to the other ^{19}F resonances, this signal is found to shift upfield after oxidation (Figure 2). Moreover, in both the reduced and oxidized forms the resonance moves further upfield with decreasing temperature (Figure 4), while the signals have relatively short T_1 relaxation times (Table 2). This suggests that this ^{19}F nucleus lies in close proximity to the paramagnetic cluster; however, the ^{1}H resonances from the hyperfine-shifted signals of oxidized 3-F-Phe HiPIP show no visible change from that of the native HiPIP at different temperatures (278 and 303 K; spectra not shown), and so the fluorine-labeled residues appear not to perturb the electronic structure of the cluster.

The temperature dependence for the 3-F-Tyr19 resonance in the oxidized protein shows an opposite trend to that of the 3-F-Phe66 resonance, shifting downfield with increasing temperature. This may be related to the positions of these two residues, which lie at 90° relative to the cluster.

^{19}F Longitudinal Relaxation Time. It has been generally observed in magnetic resonance studies of biological macromolecules that the decay of heteronuclear magnetization after a 180° pulse often cannot be fit by a single exponential as a result of cross relaxation (CR) from neighboring nuclei. Herein, CR between ^{19}F and ^{1}H atoms can be eliminated by continuous saturation of the proton resonances during the entire ^{19}F T_1 measurement.[11,17,23] We have found the experimental T_1 values to be independent of the method of measurement (Table 2), and so CR is not a significant contributor to relaxation. In fact, the CR contribution, σ_{FH}, can be estimated for each ^{19}F nucleus by use of eq 6,[17] where $k = \gamma_F\gamma_H h$, τ_c is the isotropic correlation

$$\sigma_{FH} = (k^2\tau_c/10r_{FH}^6)[(6/(1 + (\omega_F + \omega_H)^2\tau_c) - 1] \qquad (6)$$

time, ω_F and ω_H are the Larmor frequencies for ^{19}F and ^{1}H, and r_{FH} is the average F−H distance. Taking $\tau_c = 3$ ns (a typical value used for HiPIP[16,33]), $\omega_F = 235$ MHz, and $\omega_H = 250$ MHz, the magnitude of σ_{FH} can be estimated (see footnote to Table 6). The NOE for ^{19}F nuclei, resulting from broad-band proton decoupling, can also be estimated by use of eq 7,[17] where ρ_{FH}

$$\eta_F\{H\} = (\gamma_H/\gamma_F)(\sigma_{FH}/\varrho_{FH}) \qquad (7)$$

is the observed relaxation rate from T_{1obs} ($\rho_{FH} = 1/T_{1obs}$) in Table 2, which includes both the diamagnetic and paramagnetic contributions. The calculated NOE's are also listed in Table 6. It is clear from Table 6 that, with the exception of the ^{19}F

(27) Bertini, I.; Capozzi, F.; Ciurli, S.; Luchinat, C.; Messori, L.; Piccioli, M. *J. Am. Chem. Soc.* **1992**, *114*, 3332.
(28) Gaillard, J.; Albrand, J.-P.; Moulis, J.-M.; Wemmer, D. E. *Biochemistry* **1992**, *31*, 5632.
(29) Nettesheim, D. G.; Harder, S. R.; Feinberg, B. A.; Otvos, J. D. *Biochemistry* **1992**, *31*, 1234.
(30) Cammack, R. *Biochem. Biophys. Res. Commun.* **1973**, *2*, 548.

Table 5. Solvent Isotope Effect on ^{19}F Chemical Shifts

	Phe(−1) (Δδ, ppm)			Phe48 (Δδ, ppm)			Phe66 (Δδ, ppm)			Tyr19 (Δδ, ppm)
	2-F	3-F	4-F	2-F	3-F	4-F	2-F	3-F	4-F	3-F
red, $\delta(H_2O) - \delta(D_2O)$	0.10	0.12	0.11	0.06	0.06	0.05	0.03	0.01	0.01	0.02
ox, $\delta(H_2O) - \delta(D_2O)$	0.13	0.09	0.11	0.04	0.12	0.13	0.00	0.07	0.06	0.01

[a] Shifts greater than 0.1 ppm correspond to a frequency change of more than 23.5 Hz, which is readily detectable and indicative of a bona fide isotope effect.

Table 6. Estimated NOE's for ^{19}F ($\eta_F\{H\}$)

assgnt	ρ_{FH}[a]	$\eta_F\{H\}$ (%)[b]
2-F-Phe 48	15.4	-4.5
2-F-Phe 66	9.2	−7.5
3-F-Phe 48	4.3	−16.1
3-F-Phe 66	27.0	−2.6
4-F-Phe 48	1.7	−40.7
4-F-Phe 66	10.0	− 6.9
3-F-Tyr 19	17.5	−3.9

[a] ρ_{FH} is the relaxation rate ($1/T_{1obs}$). [b] $\eta_F\{H\}$ was calculated from eq 7, where σ_{FH} (=−0.65 s^{-1}) was calculated from eq 6 for distances (r_{FH} = 2.5 Å) to the vicinal aromatic hydrogens. Use of distances from ^{19}F to the nearest ^1H in space gives rise to smaller expected NOE's.

resonances from 3-F and 4-F-Phe 48, the cross-relaxation rate is, on average, 5−40 times slower than the spin−lattice relaxation rates, and therefore the observed NOE's are less than 10% in magnitude. These estimates are in good agreement with the experimental results summarized in Table 6 and Figure 5.

The CSA contribution to the ^{19}F relaxation is expected to be small for HiPIP. The correlation time (τ_c) for HiPIP is in the range 10^{-9}−10^{-8} s. Theoretical calculation shows that the relaxation time from CSA is greater than 0.6 s at 235 MHz for a ^{19}F nucleus.[11] This relaxation time is significantly longer than the observed relaxation time for most ^{19}F nuclei in fluorinated HiPIP.

Both the variation of the ^{19}F chemical shift in Figure 2, and the ^{19}F solvent isotope data in Table 5, suggest that the protein undergoes a minor conformational change after cluster oxidation. This is consistent with recent NMR solution structural studies of *C. vinosum* HiPIP by Bertini and co-workers.[31] The effect of the conformational change is also reflected in the longitudinal relaxation times. The changes in relaxation times for each redox pair do not follow a consistent pattern (T_{1obs} in Table 2). If the change in the paramagnetism of the cluster were the only factor involved, then the change in the paramagnetic contribution to relaxation should change in an analogous fashion (that is, increase or decrease) for each of the ^{19}F nuclei, as previously observed for T_1 measurements of cysteine protons.[22,26,27] Since the paramagnetic contribution to relaxation also depends on the distance (r^{-6}) from the relevant nuclei to the cluster, the possible change in orientation of the fluorine-labeled side chain should be taken into account. For the ^{19}F nucleus of 3-F-Tyr19 the relaxation time increases from an average of 40 ms for the reduced state to 57 ms for the oxidized state. Since the electronic relaxation of the oxidized cluster is rapid, and does not promote efficient relaxation of neighboring nuclei, the observed increase in relaxation time most likely reflects both this decrease in relaxation efficiency and the movement of Tyr19 away from the cluster after oxidation.[2b,4] Other sources of relaxation for the ^{19}F nuclei include the dipolar interaction with neighboring protons and solvent (if any). This relaxation pathway also depends on the orientation of ^{19}F nuclei in the protein, and so the increased relaxation time of the ^{19}F nucleus in 3-F-Tyr may reflect a change in the contact interaction of the fluorine with neighboring nuclei. The relaxation time of the signal at −40.3 ppm from 4-F-Phe48 is the longest observed in either the reduced or oxidized forms. Crystallographic studies show that Phe48 is located close to the surface of the protein and that C-4 of Phe48 lies farthest from the cluster. The more than 3-fold increase in relaxation time following oxidation cannot be explained by the increased paramagnetism of the cluster. Previously, it has been observed that the relaxation times for fluorine-labeled proteins increases with solvent exposure.[10,11,17,23,25] The longer relaxation times observed for the ^{19}F nuclei of 3-F-Phe48 (−37.1 ppm) and 4-F-Phe48 (−40.3 ppm) (Tables 2 and 3) most likely reflects a conformational change of the peptide chain after oxidation of the cluster that results in increased solvent accessibility. This is consistent with the isotope shifts summarized in Table 5. The shorter relaxation time for the ^{19}F resonance of 3-F-Phe66 (Table 3) after oxidation may be taken as additional evidence (along with its unusual temperature dependence) for a close interaction with the cluster.

Conclusions

Fluorine-19 NMR provides an excellent probe of redox-dependent conformational changes in electron-transfer proteins. This should be of particular value for evaluation of structural perturbations in mutant proteins. Similarly, evaluation of solvent isotope effects on ^{19}F chemical shifts provides a probe of solvent accessibility to the protein core in both native and mutant HiPIP's. For HiPIP we have rationalized the oxidation-state-dependence of the fluorine chemical shifts and relaxation times in terms of a diamagnetic conformational change of the polypeptide chain rather than pseudocontact shift contributions from the cluster. Fluorine-19 NMR also affords a convenient test of the relative contribution of cross-relaxation to magnetization decay. The small observed NOE's for the ^{19}F resonances indicate that cross relaxation between ^1H and ^{19}F is small and is consistent with the similarity in ^{19}F T_1 results obtained with and without proton decoupling. The unusual temperature dependence and fast relaxation times of 3-F-Phe66 and 3-F-Tyr19 ^{19}F resonances most likely reflect a close interaction of these two residues with the iron−sulfur cluster.

Acknowledgment. We thank Ivano Bertini and Claudio Luchinat for valuable comments. This work was supported by the National Science Foundation (Grant CHE-8921468). J.A.C. is a Fellow of the Alfred P. Sloan Foundation, a Camille Dreyfus Teacher-Scholar, and a National Science Foundation Young Investigator.

IC951159T

(31) Banci, L.; Bertini, I.; Dikiy, A.; Kastrau, D. H. W.; Luchinat, C.; Sompornpisut, P. *Biochemistry* **1995**, *34*, 206−219.
(32) Przysieck, C. T.; Meyer, T. E.; Cusanovich, M. A. *Biochemistry* **1985**, *24*, 2542.
(33) Banci, L.; Bertini, I.; Carloni, P.; Luchinat, C.; Orioli, P. L. *J. Am. Chem. Soc.* **1992**, *114*, 10683.